Geophys. J. Int. (1991) **105,** 491–502

The deep structure of Gorringe Bank (NE Atlantic) and its surrounding area

Andrée Bergeron* and Jean Bonnin
Institut de Physique du Globe 5, Rue René Descartes, F-67084 Strasbourg Cedex, France

Accepted 1990 December 10. Received 1990 December 10; in original form 1989 December 28

SUMMARY

The structure and origin of the disturbed oceanic area southwest of Cape São Vicente (south Portugal) is still a matter of debate. What are the reasons for such a huge relief and for the high positive free-air anomaly? To go further in the understanding of this atypical region, the deep structure has been investigated by means of 3-D gravity modelling, taking into account other geophysical and geological information such as seismic reflection data. The results clearly show that all topographic highs are associated with shallow Moho, and are consequently not isostatically balanced. Gorringe Bank is shown to be strongly asymmetrical and to be associated with a major fracture within the lithosphere. Considering the geodynamical context of this area the mechanical equilibrium could be due to a distribution of vertical stresses; an estimation of the required stresses is given showing no major evidence that this is impossible.

Key words: deformation, gravity, isostasy, North Atlantic, oceanic lithosphere.

INTRODUCTION

In the northern Atlantic Ocean, 4° west of Gibraltar, one observes a succession of massive linear ridges and of deep and narrow abyssal plains (Fig. 1). One of those ridges, Gorringe Bank, periodically arouses the interest of the scientific community. Indeed, it poses questions in several domains to the Earth scientist.

The geologist finds there unusual outcropping rocks. Sample analysis (Honnorez & Fox 1973; Gavasci, Fox & Ryan 1973; Hékinian, Bougault & Pautot 1973; Ryan, Hsü *et al.* 1973; Prichard 1979; Cornen 1982; Prichard & Cann 1982) and *in situ* observations by submersible (Auzende *et al.* 1978, 1979, 1982, 1984; Le Lann, Auzende & Olivet 1979; Lagabrielle & Auzende 1982) have shown that one passes almost continuously from the upper mantle rocks composing Mount Gettysburg (the western peak of Gorringe Bank) to the gabbros and alkaline basalts of Mount Ormonde (the eastern peak), and thus that an almost continuous section of the oceanic crust and upper mantle is exposed. Therefore, Auzende *et al.* (1978, 1979) consider Gorringe Bank as a portion of uplifted and tilted oceanic lithosphere, with a possible occurrence for the tilt at the time of anomaly J (110 Myr BP), known to correspond to an important phase of northern Atlantic history (Olivet *et al.* 1984). The weak point of this interpretation remains that the oceanic sequence has not yet been completely sampled, since on the contrary an unconformity between gabbros and peridotites has been observed (Auzende *et al.* 1982).

Fukao (1973), studying the 1969 February 28 large earthquake and its aftershocks, is also led to the hypothesis of an uplifted block. However, for the seismologist also this area is somewhat unusual: the distribution of epicentres, roughly linear along Gloria Fault (central part of the Azores–Gibraltar line), becomes scattered east of 18°W (Fig. 1); very large shocks occur (e.g. for the above-mentioned event, $Ms = 7.9$—Fukao 1973) but little lower activity is reported; this ocean–ocean convergence (Minster & Jordan 1978; Olivet *et al.* 1984) is characterized by a very low rate of convergence and is not associated with any Benioff 'plane'; the focal solutions (e.g. McKenzie 1972; Udias, Lopez Arroyo & Mezcua 1976; Grimison & Chen 1986, 1988) show a combination of thrust faulting and strike–slip motion, without any conspicuous pattern for the distribution of the nodal planes but a noticeably consistent subhorizontal NNW–SSE direction of the *P*-axes (Grimison & Chen 1986); trying to define precise plate boundaries, one is led to difficulties such as the individualization of a Gorringe 'miniplate' (Purdy 1974); so that, rather than a sharp plate boundary, one may think of the convergence of the two large plates Africa and Europe which induces deformations over a broader area (Bonnin 1978; Grimison & Chen 1986).

*Now at: Palais de la Découverte, Avenue Franklin Roosevelt, F-75008 Paris, France.

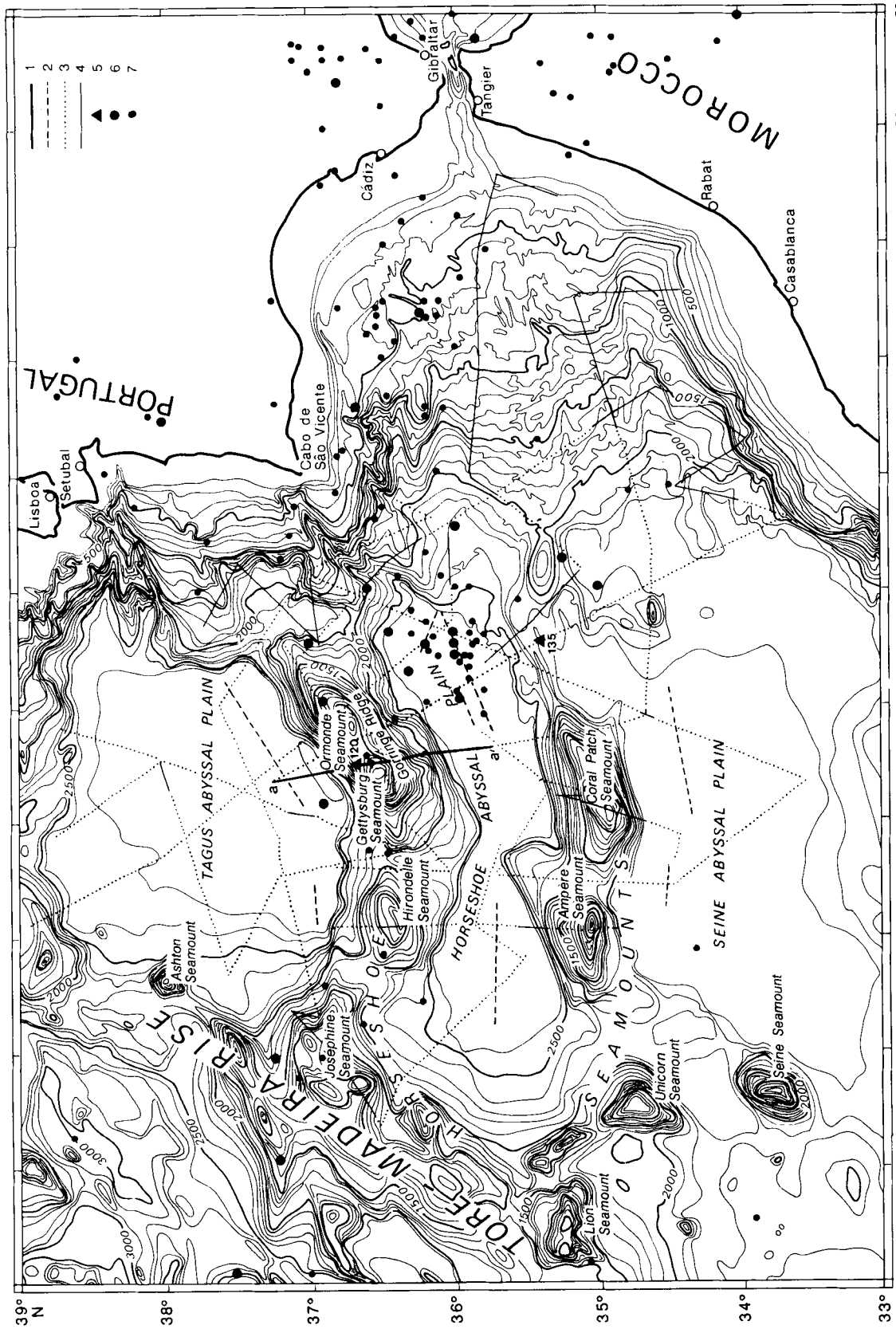

Figure 1. General map: bathymetry in corrected fathoms from Laughton *et al.* (1975), contour interval 100 fathoms. (1) Location of section NESTLANTE I 11 (see Fig. 3). (2) Refraction lines used for the determination of velocities (see Table 1). (3) Seismic reflection sections used to determine the shape of sediments (surveys NESTLANTE 1, GIBRACO, ALBATLANTE, TRIPOD and NORESTLANTE II of Institut Français de Recherche pour l'Exploitation de la Mer). (4) Sections interpreted but not shown in this study. (5) DSDP sites. (6), (7) Epicentres of seismic events from 1904 to June 1988 (data from European–Mediterranean Seismological Centre, with permission): (6) $M \geq 5$, (7) $M < 5$.

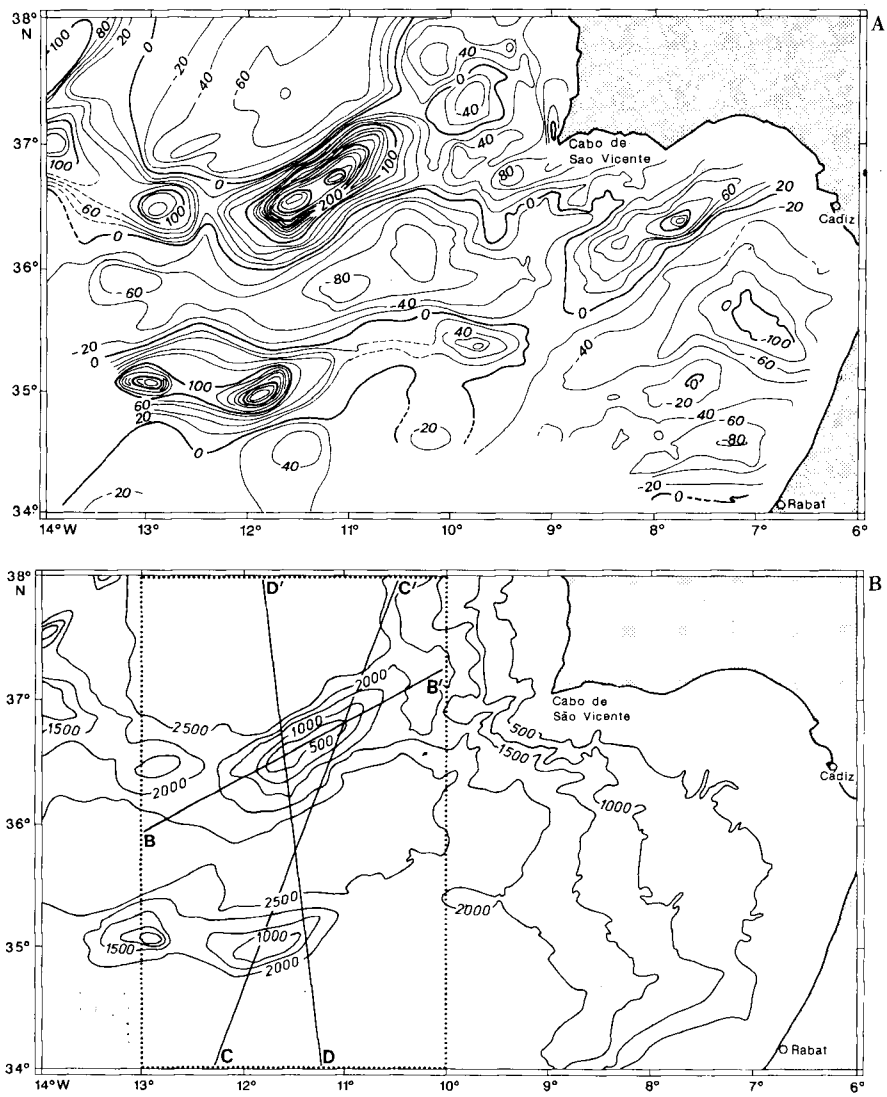

Figure 2. (A) Free-air anomaly in milligals (from Bonnin 1978). Contour interval 20 mgal. This chart has been obtained by adding data of cruises GIBRACO and ALBATLANTE to Purdy's (1975) chart, which in turn was an extension of the Admiralty chart C6101A. In comparison to Purdy's chart the present one differs mostly by the addition of data in the Tagus Abyssal Plain. This does certainly not have much influence on the general quality of the gravity data. Histograms of cross-over errors for the free-air anomaly gravity data are shown in Purdy (1975, fig. 9, p. 985). (B) Simplified topography (from Laughton *et al.* 1975) of the area shown on Fig. 2(A); contour interval 500 fathoms. The box shows the area represented on Figs 4, 5 and 7. BB', CC", DD': location of sections shown on Figs 6 and B1.

Finally, the gravity field associated with this sharp relief is highly anomalous, the geoid (Souriau 1984) as well as the free-air anomaly (Fig. 2) which reaches a huge maximum ($+368$ mgal $= 368 \times 10^5$ m s^{-2}) over Mount Gettysburg and is one of the world's largest positive free-air anomalies. It is worth emphasizing that the pattern of anomalies (short-wavelength anomalies strongly correlated with the relief) disqualifies too deep sources. These gravity data gave rise to various interpretations: Le Pichon (in Le Pichon, Bonnin & Pautot 1970), Purdy (1974, 1975), Purdy *et al.* (1975, personal communication), Souriau (1984). Those models are all focused on Gorringe Bank and, except Souriau's one, they agree on the asymmetry of Gorringe Bank. The disagreements come from the answer to the following two questions:

(i) is there a subduction *sensu stricto* under Gorringe Bank?

(ii) is Gorringe bank in a state of local isostatic equilibrium?

Two attempts were made to take into account a subduction: Le Pichon (in Le Pichon *et al.* 1970) and Purdy (1975). Even if we disregard the fact that there is clearly no Benioff 'plane' there, none of these interpretations could propose a simple working for the subduction: Le Pichon assigns two different polarities to the subduction, and Purdy's model involves a mechanical decoupling within the lithosphere. A local isostatic equilibrium is assumed by Souriau (1984): as a consequence, the compensating masses extend down to 60 km depth and Souriau herself notes that 'the setting up of a low density root at such great depth raises some difficulties'. Two other models (Purdy 1975; Purdy *et al.* 1975, personal communication) have been proposed which explain the positive anomaly by introducing a high-density material at low depth under Gorringe Bank, which in turn

implies that Gorringe Bank is out of isostatic equilibrium. Many arguments exist to assert that this region is (Minster & Jordan 1978) and has been for a long time (Olivet *et al.* 1984), submitted to deformations; it is thus possible to imagine that the prevailing stress distribution satisfies the mechanical equilibrium of this structure.

OBJECTIVES AND METHODS

It follows from the above introduction that both the origin and the state of equilibrium of Gorringe Bank are still open questions. To go further in the understanding of this feature, two elements should be useful:

(i) a better knowledge of the deep structure of Gorringe Bank and of its neighbourhood; and
(ii) a better knowledge of the seismicity in this area.

Some improvement concerning the second point should come from the installation of ocean-bottom seismometers by the University of Lisbon (Simoes, Baptista & Mendes-Victor 1989). In the present paper we are interested in the first point.

In our case the gravity signal is strong enough to let us have a good hope of obtaining significant information on the deep structure; moreover, several thousand kilometres of seismic reflection profiles are available (Fig. 1), and results of seismic refraction (Fig. 1) have been published (Purdy 1975; Bonnin 1978), which gives us the opportunity to compute the gravity signature of the uppermost sources so as to evidence the part of the signal due to deeper ones. It remains then to determine these deep sources. What can we expect in solving this gravity inverse problem? It goes without saying that no unique solution exists; but neither does it usually to inverse problems in geophysics. Therefore, unless additional information gives good constraints, one must not try to exhibit a definitive model from gravity data analysis. This inherent ambiguity in the gravity inverse problem may be responsible for the usual mistrust affecting gravity modelling. Gravity is nevertheless a useful tool that must not be discarded too fast. With a good control on the different steps and assumptions, and taking into account the possible ranges of the parameters involved, we can define a set of 'physically possible' solutions. Then, if stable characteristics can be evidenced on those solutions, they are most likely characteristics of the actual structure.

DATA REDUCTION

From now on, all gravity calculations referred to are 3-D. There are two main reasons for that: (i) the hypothesis of a cylindrical source body, assumed in any 2-D model, may hardly be justified here due to the size of the structures (Fig. 1); (ii) there are no reasons to look for an interpretation restricted to Gorringe Bank: the other topographic highs, though not so famous, have much in common with Gorringe Bank. Our computations, direct as well as inverse, are based on Cordell & Henderson's (1968) method. For direct calculations, the body involved is approached by means of a bundle of elemental, rectangular prisms with a square section centred on the nodes of a regular grid. At each grid node, the contribution of every prism is calculated; the total effect of the body is obtained by summing up all elemental contributions.

The sedimentary cover in this area has a very variable thickness: it reaches in places more than 5 km, while it is almost nothing over the topographic highs. It may thus significantly affect the gravity field. For a rough preliminary estimation, assuming a $2.67 \times 10^3\,kg\,m^{-3}$ Bouguer density (as is commonly accepted), a $0.3 \times 10^3\,kg\,m^{-3}$ mean density contrast between crust and sediments (i.e. a $2.37 \times 10^3\,kg\,m^{-3}$ density for the sediments), and assuming that the infinite slab Bouguer correction applies in the plains, one finds a significant 65 mgal contribution to the gravity effect of the simplified sediment layer where this assumption makes sense (in the vicinity of the centres of the plains); the corresponding contribution vanishes outside the plains. We decided therefore to extend the reductions to the sedimentary bodies. One computes the straightforward Bouguer anomaly, which practically cancels the contribution from topography if the Bouguer density is close enough to the actual crustal density, and then repeats the process, but starting from the classical (topography) Bouguer anomaly and correcting for the geometry and density of the first sedimentary layer instead of the geometry and density of the water layer. This process is then iterated for the next sedimentary layer, and so on until the last sedimentary layer (i.e. the one located just above the acoustic basement). The anomaly obtained that way is obviously shifted toward the positive values due to the excess of mass introduced. To concentrate on the significant variations of the anomaly (i.e. its relative variations) one removes the effect of a slab, the mass of which is equal to the excess mass. Here the slab must have a horizontal extension limited to the grid surface so as to minimize the edge effects. The anomaly obtained then has a mean value close to zero and is therefore directly comparable to the free-air anomaly; we called it 'reduced anomaly'.

The topography, on the one hand, and the free-air anomaly, on the other, have been digitized (topography from Laughton, Roberts & Graves 1975; gravity from Bonnin 1978) and gridded ['thin plate' spline interpolation (Thomann 1970); for other details on spline interpolation methods see also Gonzalez-Casanova & Alvarez (1985)]. The shape of the sedimentary bodies has been derived from seismic reflection profiles. The six stratigraphic sequences distinguished (Fig. 3) are delimited by reflectors (with one exception) that correspond to major tectonic unconformities. The reflection profiles have been sampled every 1/2 hr (i.e. approximately 5 km) along the ship's tracks; the two-way traveltimes have been transformed into kilometres, using velocities estimated from seismic refraction results (Purdy 1975; Bonnin 1978—see Appendix A), and finally interpolated ('thin plate' spline interpolation, see above) to obtain the vertical position of each sedimentary discontinuity on the same regular grid as for topography and gravity. The extent of the grid (34°N–38°N; 10°N–13°W) and the grid step (10 km) have been chosen so as to offer a good compromise between the distribution of data (both seismic and gravity) and the dimensions of the topographic structures (e.g. roughly 80 km wide, 150 km long, 5 km high for Gorringe Bank). The locations of the reflection profiles and of the refraction lines are shown on Fig 1; refraction data are presented and discussed in Appendix A.

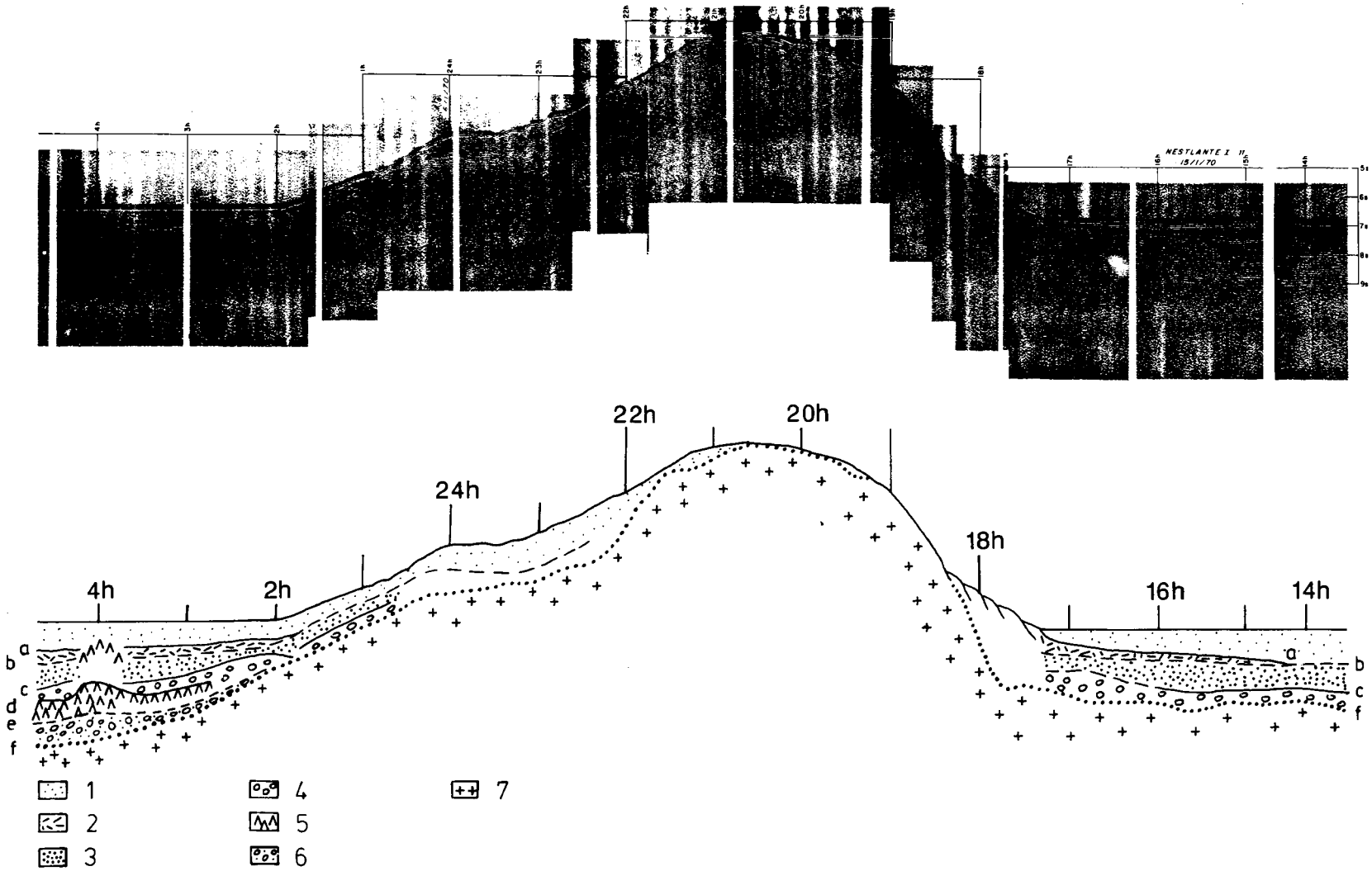

Figure 3. Section NESTLANTE I 11 (location given in Fig. 1); this section crosses, from right to left, the Horseshoe Abyssal Plain, Mount Gettysburg and the Tagus Abyssal Plain. Note the thin sediments over the relief. (1) Recent turbiditic series. (2) Apron; these opaque series can be observed on the margins west of Gibraltar and in the western parts of the Horseshoe Abyssal Plain and the Seine Abyssal Plain; they have been interpreted as sediment slides equivalent to those existing in Rharb and in Guadalquivir (Bonnin, Olivet & Auzende 1975). (3) Oligo-Miocene series; the top of these series (b on the figure) is an unconformity which corresponds to a hiatus of sedimentation at the Miocene period. (4) Cretaceous series; here again the top of these series (c on the figure) corresponds to an unconformity: the Eocene discordance. (5) Anhydritic layer. (6) Subsalt layer. (7) Acoustic basement. All the sedimentary bodies (1 to 6) are limited by reflectors (a to f) the positions of which have been measured on the sections, with the exception of the limit anhydrite/subsalt (e) which has been arbitrarily placed (see text). The diapirs (e.g. at 4h on the figure) are due to a halite layer which has not been taken into account in the gravity computations due to its probably restricted size (Bergeron 1988).

Only interface (e) (Fig. 3) has not been obtained that way, but directly calculated from the interpolated interfaces (d) and (f). The existence of an subsalt layer is inferred from geological (Auxiètre & Dunand 1978; G. Nély, personal communication) and geophysical (Bergeron 1988) observations. Such a layer, most likely made of sandstone (Auxiètre & Dunand 1978), should correspond to a velocity inversion and thus it would not show up in the refraction data; moreover it is overlaid by salt, an opaque series, and could thus hardly be seen on the reflection profiles.

Knowing the shape of the sedimentary bodies one can calculate their gravity signature, provided densities are known; in fact what is important is the contrast between crustal and sedimentary densities, so that one must choose the crustal density and the respective sedimentary densities. Since: (i) no direct measurement of the crustal density is available; (ii) refraction data do not permit a non-speculative choice of the crustal density (Purdy 1975), but suggest that the latter may be rather low (Purdy 1975); (iii) a $0.1 \times 10^3\,\mathrm{kg\,m^{-3}}$ increase (resp. decrease) of the crustal density should induce some 40 mgal decrease (resp. increase) in the peak to peak amplitude of the reduced anomaly, the computations have been finally conducted for five different values of the crustal density covering the 'physically probable range' (2.5–$2.9 \times 10^3\,\mathrm{kg\,m^{-3}}$). The sedimentary densities have been chosen using the empirical velocity/density relationship of Nafe & Drake (1963), which is up to now the only alternative to direct measurements; we considered it unacceptable to ignore the scatter of this plot, given that it may provoke a significant deviation of the densities and thus of the gravity effect (e.g. for $V_P = 2.0\,\mathrm{km\,s^{-1}}$, the relative variation allowed for density is 17 per cent, which corresponds to 40 per cent when converted to density contrast). The computations have therefore been done for three different sets of densities ('upper', 'mean' and 'lower', picked from the Nafe & Drake's plot, see Table A3 in Appendix A); together with the possible range of the crustal density, the reduced anomaly has been computed for 15 different cases covering the 'physically probable range' of the parameters.

DEEP SOURCES OF ANOMALOUS GRAVITY FIELDS

An example of reduced anomaly is shown on Fig. 4. The amplitude of the reduced anomaly is always roughly half the amplitude of the straightforward Bouguer anomaly, which has in turn half the amplitude of the free-air anomaly. This is an *a posteriori* confirmation of the interest of such reductions. Finally, the reduced anomaly still shows significant variations, of the order of 100 mgal. The topographic highs are always associated with positive values of the reduced anomaly, which is roughly linear over Gorringe Bank, and shows a complex pattern over Coral-Patch (Fig. 4). Of course, the values chosen for the different densities have influence (Bergeron 1988; see Appendix B), but, within the allowed ranges, the general features prevail clearly, and the consequence is that we have to admit the existence of deeper seated sources, since at this step all information on the uppermost part of the structures has been taken into account. If we consider the wavelength of the remaining signal (Fig. 4), the deep sources cannot

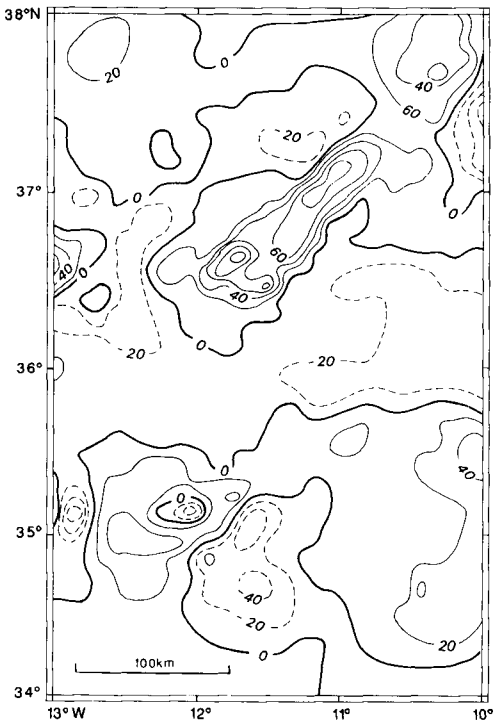

Figure 4. Reduced anomaly in milligals, contour interval 20 mgal. The value of crustal density is $2.7 \times 20^3\,\mathrm{kg\,m^{-3}}$ and 'mean' values are taken from Nafe and Drake's plot. Solid lines show positive (dashed lines negative) values of the reduced anomaly. See the text for discussion. Location shown in Fig. 2(B).

consist of small heterogeneities that would not have been detected by the seismic experiments, neither could they be seated too deep (not more than 25 km). Moreover, they have to correspond to an actual mass distribution within the lithosphere; if we assume that it could correspond to a surface delimiting two different density media, a natural candidate is the Moho discontinuity.

Refraction data (Purdy 1974, 1975) and wave propagation analysis (Cara & Hatzfeld 1976, 1977; Marillier & Mueller 1982; Kuo, Forsyth & Wysession 1987) have shown that the upper mantle shows here low velocities, thus low density. We arbitrarily have taken 3.15 and $3.3 \times 10^3\,\mathrm{kg\,m^{-3}}$ as two possible values for the upper mantle density. After smoothing the reduced anomaly to remove the high frequencies, we have made 3-D inverse calculations for several sets of values of the parameters (densities, mean depth of sources) using Cordell & Henderson's (1968) iterative method. The mean depth of the sources has been imposed taking advantage of the refraction data (Purdy 1974, 1975; Bonnin 1978) within a possible range from 12 to 14 km.

RESULTS

The two examples of Fig. 5 show very similar features. The computed surface is obviously strongly correlated with the reduced anomaly (Fig. 4); maxima (resp. minima) of the reduced anomaly are always associated with highs (resp. lows) of the computed surface. In particular, Gorringe Bank remains associated with a high of the computed surface, whatever the actual values of the parameters (densities,

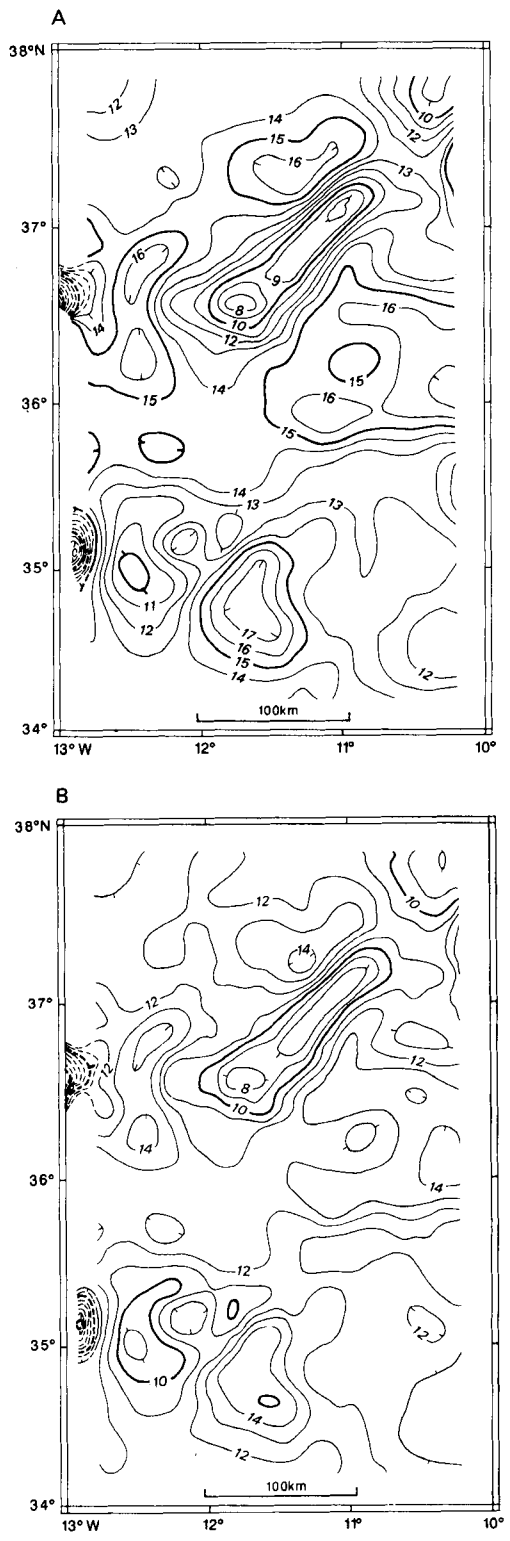

Figure 5. Two examples of the computed surface. Depths in kilometres, curve interval 1 km. Values of parameters: A: crustal density: 2.7×10^3 kg m^{-3}; sedimentary densities: 'mean'; mantle density: 3.15×10^3 kg m^{-3}; mean source depth: 14 km; B: crustal density: 2.7×10^3 kg m^{-3}; sedimentary densities: 'mean'; mantle density: 3.30×10^3 kg m^{-3}; mean source depth: 14 km. The outermost part of the zone is not represented since it is highly affected by edge effects; however, in places where the behaviour of the computed surface seemed consistent enough, the isobaths have been represented by dashed lines.

mean source depth), taken within the 'physically probable ranges'; thus, there must exist a high density body close to the sea-bottom surface within Gorringe Bank. The effects of the possible variations of the parameters (Bergeron 1988) can be summarized by saying that the lower the density contrast between crust and upper mantle, and/or the deeper the mean source depth, and/or the higher the relative variations of the reduced anomaly (depending on the choice of densities), the sharper the relief of the computed surface. However, several clear constant types of behaviour are evidenced. Gorringe–Hirondelle Ridge shows a positive correlation between topography and the computed surface. This is very clear for Gorringe Bank and may also be valid for Hirondelle, though its location near the limits of the zone compels one to be cautious; the whole ridge is then out of isostatic equilibrium. Moreover, a discrepancy of some 15° between the main strikes of topography and of the computed surface is shown, the computed surface trend being rotated by 15° counterclockwise with respect to topography. Main trends of topography, of free-air anomaly, and of the reflectors mapped are all approximately 45° ± 2; the change in trend appears after the correction for topography (classical Bouguer correction) has been applied, the new trend being then 59° ± 2. We think that this trend does exist in the free-air anomaly, but is hidden by the effect of topography and of the uppermost sources. But the main argument remains that this latter direction coincides with the direction of the fractures as deduced from seismic data (Bonnin 1978) and we think therefore that it is significant. Beneath the northern flank of Gorringe Bank where a fault has already been identified within the crust, the low crustal thickness (Fig. 6) suggests that we face here a major fracture within the lithosphere; that may be related to the several periods when Gorringe Bank acted as a fracture zone (Olivet *et al.* 1984). Under Gorringe Bank, the computed surface comes as close to the sea level as 8000 m, and probably closer: the high-frequency part of the signal removed, cut off for convenience, has significantly high values only over the topographic highs; if taken into account, it may raise the computed surface in places up to 3500 m below the sea level.

As concerns Ampère–Coral-Patch Ridge, it is more difficult to conclude. Ampère Bank, though on the edges of the map, may correspond to a low zone of the computed surface and thus tend to isostatic compensation. Coral-Patch is characterized by a complex pattern of the reduced anomaly and therefore of the computed surface. The limited seismic data over Coral-Patch makes us think that the observed small-size low may more likely originate in the acoustic basement: the latter is poorly known over Coral-Patch and could present some local collapse which is not detected on the seismic reflection sections; it would have induced a default of mass not taken into account in the corrections, and led to this local disturbance of the computed surface. Anyhow, no clear correlation between the shape of the computed surface and the topography can be observed. Obviously, the plains correspond to low and quiet zones of the computed interface. In agreement with Purdy (1974), a clear difference between the two parts of the Horseshoe Abyssal Plain is shown, the eastern part being deeper than the western one (Fig. 5).

One of the main results remains that the whole

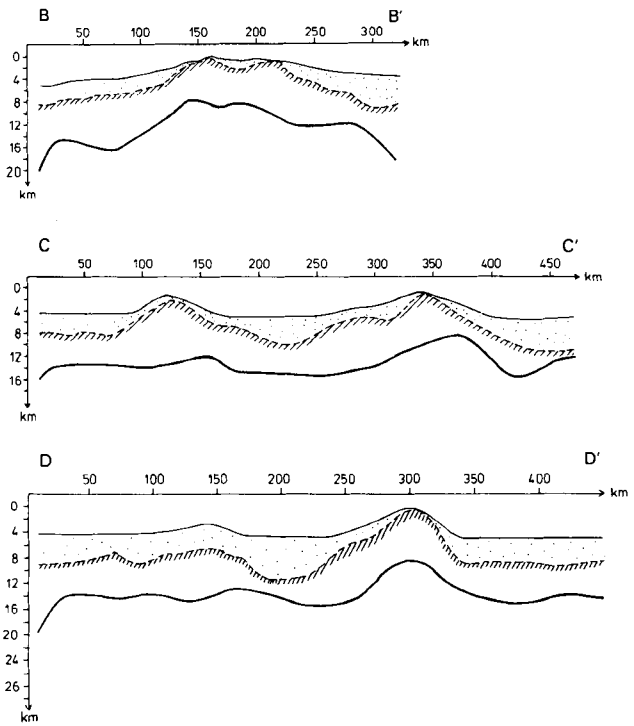

Figure 6. Three sections of the model shown on Fig. 5(A) locations given in Fig. 2(B). The structure is represented by sediments (stippled), the acoustic basement (hatched line) and the computed surface (thick line). Edge effects are visible, but restricted to the 30–40 outermost kilometres. Note the asymmetry of Gorringe Bank (section BB'), where the maximum of the computed surface is shifted with respect to topography, and the small crustal thickness beneath its northern flank (section CC").

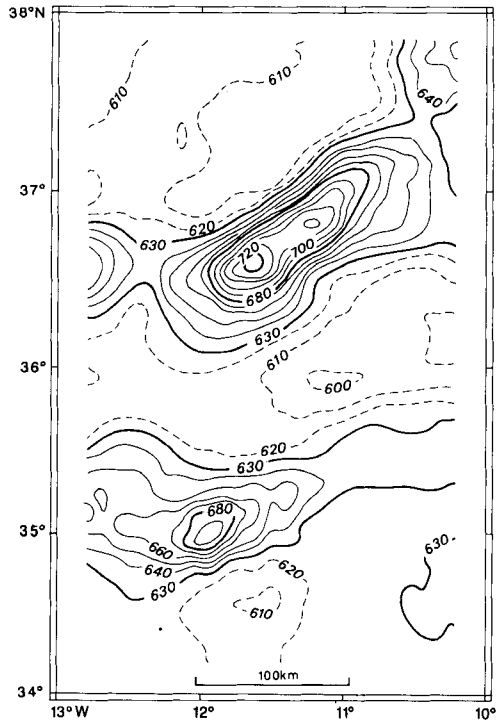

Figure 7. Pressure distribution created by the structure (case of Fig. 5A) on a horizontal plane (plane depth 25 km). Values in MPa (1 MPa = 10 bar); curve interval 10 MPa. The dashed lines represent values lower than mean pressure, solid lines values greater than mean pressure ($\langle p \rangle$ = 629 MPa).

Gorringe–Hirondelle Ridge, and to a lesser extent Coral-Patch, are associated with highs of the computed surface, which is just the opposite of what would have been expected from structures in isostatic equilibrium. Only Ampère Bank seems to be underlain by a low of the computed surface. How far from isostatic equilibrium? From our models, it is easy to compute the pressure created by the structures on a horizontal plane. The depth of the plane is chosen so that it is deeper than any discontinuity. Calculations have been done for all the models; the results are extremely stable throughout the different models: the amplitude of the variation in pressure ranges from 132 to 135 MPa and the shape of the isobars are similar. The topographic highs correspond to zones of high differential pressure (Fig. 7), and are therefore all, including Ampère Bank, not isostatically balanced. The maximum of pressure is always obtained beneath Mount Gettysburg, and the minimum beneath the eastern Horseshoe Abyssal Plain, some hundred kilometres away from the maximum. This value is not so high as to disqualify our results, especially if one keeps in mind the tectonic context of the area; kinematic reconstructions have shown indeed that the whole area around Gorringe Bank, due to convergence of the two large plates Europe and Africa, has been under compression since at least 80 Ma (Olivet *et al.* 1984), and this is still presently the case, as the seismic activity gives evidence (Grimison & Chen 1986). One can imagine that this compression generates vertical shear stresses within the lithosphere, which could be responsible for the equilibrium of the structures.

An estimate of the stresses can be obtained if we consider a block of matter and write the balance for the external forces. Consider a right prism-shaped block with a $S = a^2$ square section and a thickness h; only the differential pressure $\delta p = p - \langle p \rangle$, where $\langle p \rangle$ is the mean value of p, has to be balanced which produces a force $\delta p\, a^2$. If one assumes that constant vertical stresses are applied all over the vertical sides, the equilibrium requires that $\delta p\, a^2 = 4\tau a h$, and thus $\tau = a\delta p/4h$. To estimate τ we shall obviously take the same prisms that have been used throughout this work, with $a = 10$ km. More delicate is the choice of h. The upper limit of the blocks is of course given by topography, but in order to choose the lower limit we must estimate to which depth shear stresses can exist within the lithosphere. An estimate can be suggested by the maximum depth of earthquakes, provided it is constrained enough. The possible depth of earthquakes, approximately defined by an isotherm (e.g. Wiens & Stein 1983; Chen & Molnar 1983), increases with the age of the lithosphere and it is not surprising to find here focal depths greater than 30 km (Fukao 1973; Grimison & Chen 1988) or even 40 km (Grimison & Chen 1986). 30–40 km seems then to be a minimum depth for the base of the blocks. Assuming 30 km, the computations show that stresses of the order of 9 MPa within Gorringe Bank are sufficient to hold it up. Note that if such a stress distribution applies, the differential pressure comes to zero. If we consider now that the whole bank is a 40 km large by 80 km long uplifted block, similar considerations lead to a value of $\tau = 40$ MPa if we consider

(Fig. 7) that 90 MPa in differential pressure have to be balanced; this value is anyway an upper limit since it only involves stresses around the block and does not take into account any possible continuous stress distribution within the bank. In both cases, the value of stresses required for the differential pressure to be balanced appears reasonable.

Another attempt could consist in considering that this relief is due to the flexion of the lithosphere. Arguments exist against such an interpretation. First, the lithosphere is probably deeply fractured in several places; this is inferred from the observations (Purdy 1975; Bonnin 1978) as well as from our results (see above) and from kinematic reconstructions (Olivet *et al.* 1984) showing that Gorringe Bank acted several times as a fracture zone. It would then be difficult to consider the lithosphere as a continuous layer, even half-infinite. Furthermore, the 2-D assumption commonly accepted in the flexure models is hardly justified here owing to both the size of the structures and the vicinity of the continents. Nevertheless, we tested the elastic flexured lithosphere model in two cases: (i) a vertical deflection is imposed at the origin so as to match Gorringe topography; and (ii) a bending moment, that could represent a vertical loading, is imposed at the origin. In both cases, an elastic thickness of the order of 10–20 km is required to obtain the appropriate wavelength, which is, away from all possible controversies, a much too low value for such an old lithosphere (more than 100 Ma, see e.g. Féraud *et al.* 1986; Prichard & Mitchell 1979).

We shall not go further with the flexured plate models; even with a more complex rheology, it could only lead to an explanation, if any, for one of the ridges, Gorringe Bank for instance. It should hardly be justified to take only Gorringe Bank into account if one considers the many characteristics that it has in common with Ampère–Coral-Patch Ridge. In addition, the fact that Ampère Bank, though underlain by a low of the computed surface, is not compensated (Fig. 7) means very likely that the compression, that affects today mostly Gorringe Bank, has formerly been accomodated, at least partly, by Ampère Bank. Finally, the fracturing of the medium has to be taken into account, which is not compatible with such flexure models.

CONCLUSION

The analysis of gravity data leads to very consistent features of the 'physically possible' solutions. It clearly shows that, except by assigning unrealistic values to the parameters, one must admit the existence of high-density bodies close to the sea-bottom surface within Gorringe Bank and the other neighbouring topographic highs, with the exception of Ampère Bank. The asymmetry of Gorringe Bank is shown to affect also its deeper parts, the main trend of which is deviated by 15° with respect to topography. The low crustal thickness beneath the northern flank of Gorringe Bank gives arguments for the existence of a major fracture within the lithosphere.

Our results open again the problem of the equilibrium and of the origin of such structures. If the elastic flexure plate model obviously does not apply, the evaluation of vertical shear stresses required for ensuring the mechanical equilibrium does not raise major physical difficulty; on the other hand the rather low values obtained encourage us to go further in that direction. What could be the mechanism responsible for the existence of such unusual structures? One must keep in mind the following elements:

(i) there, Africa and Europe (Iberia) have converged slowly since at least 80 Ma (Olivet *et al.* 1984);

(ii) this convergence today does not create any Benioff 'plane', neither is the seismic activity located on a narrow band;

(iii) from kinematic studies (Olivet *et al.* 1984), one knows that the Azores triple junction acts alternatively as a Ridge–Ridge–Ridge and as a Ridge–Ridge–Fault (present case), which corresponds in the case of Gorringe Bank to alternating between working in transform fault and in compression mode;

(iv) on Gorringe Bank, as probably on Ampère–Coral-Patch Ridge, evidence for vertical movements exists (Pastouret *et al.* 1980); and

(v) the Horseshoe Seamounts area is only part of a broader deformed zone off-shore from the Iberian and African margins.

It is thus highly probable that the deformation induced by the convergent movement of the two large plates involves there a broader zone than it usually does. The main part of the deformation should nevertheless be concentrated near the Horseshoe Abyssal Plain, as indicated by the huge relief and the many fractures evidenced. It seems that presently mostly Gorringe Bank is concerned, but Ampère Bank should have played a role formerly. Why does no real subduction exist there? The reasons could be sought in the vicinity of the continental 'collision', in the slow convergence velocity (Purdy 1975), or in the similarity of the two oceanic lithospheres (Grimison & Chen 1986). Under such hypotheses, no real 'plate boundary' exists, but better a 'boundary zone'. A precise modelling of the deformation should take into account the fracturing of the lithosphere and (as a boundary condition?) the close continental lithosphere; owing to the respective positions of the continental blocks and of the oceanic lithospheres, it could only be 3-D modelling.

ACKNOWLEDGMENTS

This work has been made possible by a grant from Ministère de la Recherche et de la Technologie, and by the financial support of Institut Français de la Recherche pour l'Exploitation de la Mer (contracts no 85-2-410398 DERO/GM 'Déformation de la lithosphère et cinématique' and no. 84/7603 'Etude et modélisation du comportement thermique et rhéologique de la lithosphère'). We wish to thank A. Blanck and G. Rheim for drawing the figures and two anonymous referees for improving our English and making useful comments. This paper was written while the first author was in post-doctoral stay at the Institut of Geophysics of the University of Kiel (Germany), with the financial support of the Commission of the European Communities (contract SC1-00098, program SCIENCE).

REFERENCES

Auxiètre, J. L. & Dunand, J. P., 1978. Géologie de la marge ouest-ibérique (au Nord de 40°N): le banc de Galice, les

montagnes de Vigo, de Vasco da Gama et de Porto. Relations avec l'ouverture de l'Atlantique Nord, *Doct. Thesis,* Université Pierre et Marie Curie, Paris.

Auzende, J. M., Charvet, J., Le Lann, A., Le Pichon, X., Monteiro, J. H., Nicolas, A., Olivet, J. L. & Ribeiro, A. (group CYAGOR I), 1978. Sampling and observation of oceanic mantle and crust on Gorringe Bank, *Nature,* **273,** 45–49.

Auzende, J. M., Charvet, J., Le Lann, A., Le Pichon, X., Monteiro, J. H., Nicolas, A., Olivet, J. L. & Ribeiro, A. (group CYAGOR I), 1979. Le banc de Gorringe: résultats de la campagne CYAGOR (Août 1977), *Bull. Soc. géol. France,* series 7, **21,** 545–556,

Auzende, J. M., Cornen, G., Juteau, T., Lagabrielle, Y., Lensch, G., Mével, C., Nicolas, A., Prichard, H., Ribeiro A. & Vanney, J. R. (group CYAGOR II), 1982. The Gorringe Bank: first results of submersible expedition CYAGOR II, *Terra Cognita,* **2,** 123–130.

Auzende, J. M., Cornen, G., Juteau, T., Lagabrielle, Y., Lensch, G., Mével, C., Nicolas, A., Prichard, H., Ribeiro, A. & Vanney, J. R. (group CYAGOR II), 1984. Géologie du banc de Gorringe, Campagne CYAGOR II, 25 Mai–18 Juin 1981, *Publ. CNEXO,* Serie Résultats des Campagnes à la Mer, vol. 27, Brest.

Bergeron, A., 1988. La région des monts du Fer-à-Cheval (Atlantique Nord): détermination de sa structure profonde par modélisation gravimétrique tri-dimensionnelle, *Doct. Thesis,* Université Louis Pasteur, Strasbourg.

Bonnin, J., 1978. Evolution géodynamique de la ligne Açores–Gibraltar, *Doct. Thesis,* Université de Paris VII.

Bonin, J., Olivet, J. L. & Auzende, J. M., 1975. Structure en nappe à l'Ouest de Gibraltar, *C. R. Acad. Sci. Paris,* series D, **280,** 559–562.

Cara, M. & Hatzfeld, D., 1976. Vitesse de groupe de l'onde de Rayleigh de part et d'autre de la ligne Açores-Gibraltar, *Ann. Geophys.,* **32,** 85–91.

Cara, M. & Hatzfeld, D., 1977. Dispersion des ondes de surface de part et d'autre de la ligne Açores–Gibraltar et en Afrique du Nord (périodes inférieures à 80 s). Colloque A.T.P. Géodyn. Médit. Occ. et de ses Abords, *Publ. Spéc. Soc Géol. Fr.,* pp. 757–764, Paris.

Chen, W. P. & Molnar, P., 1983. Focal depths of intracontinental and intraplate earthquakes and their implications for the thermal and mechanical properties of the lithosphere, *J. geophys. Res.,* **88,** 4183–4214.

Cordell, L. & Henderson, R. G., 1968. Iterative three-dimensional solution of gravity anomaly data using a digital computer, *Geophysics,* **33,** 596–601.

Cornen, G., 1982. Petrology of the alkaline volcanism of Gorringe Bank (Southwest Portugal), *Mar. Geol.,* **47,** 101–130.

Féraud, G., York, D., Mével, C., Cornen, G., Hall, C. M. & Auzende, J. M., 1986. Additional ^{40}Ar-^{39}Ar dating of the basement and the alkaline volcanism of Gorringe Bank (Atlantic Ocean), *Earth planet. Sci. Lett.,* **79,** 255–269.

Fukao, Y., 1973. Thrust faulting at a lithospheric plate boundary, the Portugal earthquake of 1969, *Earth planet. Sci. Lett.,* **18,** 205–216.

Gavasci, A. T., Fox, P. J. & Ryan, W. B. F., 1973. Petrography of rocks from the crestal area of the Gorringe Bank, *Initial Reports of the Deep Sea Drilling Project,* vol. 13-2, pp. 749–752, US Government & Printing, Office, Washington, DC.

Gonzalez-Casanova, P. & Alvarez, R., 1985. Splines in Geophysics, *Geophysics,* **50,** 2831–2848.

Grimison, N. L. & Chen, W. P., 1986. The Azores–Gibraltar plate boundary: focal mechanisms, depths of earthquakes, and their tectonic implications, *J. geophys. Res.,* **91,** 2029–2047.

Grimison, N. L. & Chen, W. P., 1988. Source mechanisms of four recent earthquakes along the Azores–Gibraltar plate boundary, *Geophys. J.,* **92,** 391–401.

Hékinian, R., Bougault, H. & Pautot, G., 1973. Atlantique Nord: étude préliminaire des roches de la fracture Gibbs (53° Nord) et de la zone de fracture Açores–Gibraltar, *C. R. Acad. Sci. Paris,* series D, **276,** 3281–3284.

Honnorez, J. & Fox, P. J., 1973. Petrography of the Gorringe Bank 'Basement', *Initial Reports of the Deep Sea Drilling Project,* vol. 13-2, pp. 747–749, US Government Printing Office, Washington, DC.

Kuo, B. Y., Forsyth, D. W. & Wysession, M., 1987. Lateral heterogeneity and azimuthal anisotropy in the North Atlantic determined from S–SS differential travel time, *J. geophys. Res.,* **92,** 6421–6436.

Lagabrielle, Y. & Auzende, J. M., 1982. Active *in situ* disaggregation of oceanic crust and mantle on Gorringe Bank: analogy with ophiolitic massives, *Nature,* **297,** 490–493.

Laughton, A. S., Roberts, D. G. & Graves, R., 1975. Bathymetry of the northeast Atlantic: Mid-Atlantic Ridge to southwest Europe, *Deep-Sea Res.,* **22,** 791–810.

Le Lann, A., Auzende, J. M. & Olivet, J. L., 1979. Campagne CYAGOR, submersible CYANA, 25 Juillet-21 Août 1977, *Publ. CNEXO.,* Sér Résult. Camp. Mer, vol. 17, Brest.

Le Pichon, X., Bonnin, J. & Pautot, G., 1970. The Gibraltar end of the Azores–Gibraltar plate boundary: an example of compressive tectonics, *Abstract, Upper Mantle Committee Symposium,* Flagstaff, AZ.

Marillier, F. & Mueller, S., 1982. Structure of the upper mantle in the northeastern Atlantic close to the Azores–Gibraltar ridge from surface-wave and body-wave observations, *Tectonophysics,* **90,** 195–213.

McKenzie, D. P., 1972. Active tectonics of the Mediterranean region, *Geophys, J. R. astr. Soc.,* **30,** 109–185.

Minster, J. B. & Jordan, T. H., 1978. Present-day plate motions, *J. geophys. Res.,* **83,** 5331–5354.

Nafe, J. E. & Drake, C. L., 1963. Physical properties of marine sediments, in *The Sea,* vol. 3, pp. 794–815, ed. Hill, M. N., Interscience Publishers, London.

Olivet, J. L., Bonnin, J., Beuzart, P. & Auzende, J. M., 1984. Cinématique de l'Atlantique Nord et Central, *Rapp. Sci. et Tech. no. 54,* CNEXO, Brest.

Pastouret, L., Auzende, J. M., Le Lann, A. & Olivet, J. L., 1980. Témoins des variations glacio-eustatiques du niveau marin et des mouvements tectoniques sur le banc de Gorringe (Atlantique du Nord-Est), *Palaeogeog. Palaeoclimatol. Palaeoecol.,* **32,** 99–118.

Prichard, H. M., 1979. A petrographic study of the process of serpentinisation in ophiolites and the ocean crust, *Contrib, Mineral. Petrol.,* **68,** 231–241.

Prichard, H. M. & Mitchell, J. G., 1979. K–Ar data for the age and evolution of Gettysburg Bank, North Atlantic Ocean, *Earth planet. Sci. Lett.,* **44,** 261–268.

Prichard, H. M. & Cann, J. R., 1982. Petrology and mineralogy of dredged gabbro from Gettysburg Bank, Eastern Atlantic, *Contrib. Mineral. Petrol.,* **79,** 46–55.

Purdy, G. M., 1974. A geophysical study of the eastern end of the Azores–Gibraltar Fracture Zone, *Ph D thesis,* Darwin College, Cambridge.

Purdy, G. M., 1975. The eastern end of the Azores–Gibraltar plate boundary, *Geophys. J. R. astr. Soc.,* **43,** 973–1000.

Ryan, W. B. F., Hsü, K. J., Cita, M. B., Dumitrica, P., Lort, J. M., Maync, W., Nesteroff, W. D., Pautot, G., Stradner, W. & Wezel, F. C., 1973. *Initial Reports of the Deep Sea Drilling Project,* vol. 13-2, US Government Printing Office, Washington, DC.

Simoes, J., Baptista, M. A. & Mendes Victor, L. A., 1989. Is the Iberian margin active?, *Abstract. Communication at the 25th General Assembly of the International Association of Seismol-*

ogy and Physics of the Earth's Interior, Istanbul, p. 42.
Souriau, A., 1984. Geoid anomalies over Gorringe Ridge, North Atlantic Ocean, *Earth planet. Sci. Lett.*, **68,** 101–114.
Thomann, J., 1970. Détermination et construction de fonctions splines à deux variables définies sur un domaine rectangulaire ou circulaire, *Doct. thesis,* Université de Lille.
Udias, A., Lopez Arroyo, A. & Mezcua, J., 1976. Seismotectonic of the Azores–Alboran region, *Tectonophysics,* **31,** 259–289.
UK Hydrographic Service, 1969. *Western Approaches to Straights of Gibraltar, Gravity Anomalies,* Chart C6101A.
Wiens, D. A. & Stein, S., 1983. Age dependence of oceanic intraplate seismicity and implications for lithospheric evolution, *J. geophys. Res.*, **88,** 6455–6468.

APPENDIX A

Refraction data

Table A1 shows the original refraction data. Lines A, A/R, B, B/R, C and D are taken from Purdy (1975). Lines 5-M, 6-M, 7-M were carried out during the 1972's cruise GIBRACO of IFREMER and lines M-NOR and M-NOR/R during the 1979's cruise NORATLANTE of the same institution. In both latter cases, the interpretation is due to Sichler (in Bonnin 1978).

Bonnin (1978) re-examined the refraction results in order to associate a seismic velocity with each sedimentary layer defined on reflection profiles (Fig. 3), i.e. to associate a refractor with each of the reflectors which delimitate the sedimentary layers. The refraction results are therefore expressed as two-way traveltimes and the refraction columns in seconds are then compared to reflectors on nearby profiles. When the most probable velocity has not shown up in the refraction experiments, it is verified whether it is possible to introduce a new layer with this particular velocity in the refraction column without violating the data, i.e. if it is possible to find a layer thickness which keeps the intercept. These results are presented in Table A2; more details can be found in Bonnin (1978). The consistency is

Table A2. Seismic velocities ($km\,s^{-1}$) assigned to the stratigraphic units from the refraction results (see text). '--' means that the series does not exist under the refraction line, '?' means that no clear association refractor/reflector has been possible. Locations of the lines are shown in Fig. 1, approximate coordinates are given in Table 1.

Line	Recent layer	Reflector a	Reflector b	Reflector c	Reflector d
A	2.00	--	3.45	4.90	--
A/R	1.84	--	3.45	?	5.95
B	2.00	3.10	?	?	6.10
B/R	2.00	3.10	?	?	5.50
C	2.00	--	3.45	4.11	--
D	2.35	--	3.42	4.55	--
5M	2.10	3.10	?	?	4.81
6M	2.10	--	3.50	4.85	--
7M	1.80	--	3.45	4.76	--
M-NOR	1.92	?	?	?	--
M-NOR/R	1.95	?	?	?	--

Table A3. Seismic velocities (in $km\,s^{-1}$) and densities (in $10^3\,kg\,m^{-3}$) assigned to the sedimentary bodies. ρ^-, ρ^0, ρ^+ mean respectively 'lower', 'mean' and 'upper' values from the Nafe and Drake's (1963) plot. Boldface values have not been obtained that way, but arbitrarily assigned from geological arguments (see Bergeron 1988), such as 'classical' density of anhydrite and 'classical' velocity and density of compact sandstone.

	V	ρ^+	ρ^0	ρ^-
Recent layer	2.00	1.73	1.90	2.16
Nappe	3.10	2.12	2.20	2.41
Oligo-Miocene series	3.45	2.20	2.30	2.44
Cretaceous series	4.50	2.37	2.46	2.63
Anhydrite	5.60	**2.80**	**2.80**	**2.80**
Infrasalt layer	**4.00**	**2.70**	**2.70**	**2.70**

Table A1. Original refraction data. Velocities are given in $10^3\,m\,s^{-1}$; figures underlined are velocities measured by oblique reflection; † means that it is an assumed value. Intercepts are given in seconds; underlined figures in intercept columns refer to thicknesses measured by wide-angle reflection; thicknesses are given in 10^3 m. Lines A, A/R, B, B/R, C, and D are taken from Purdy (1975); lines 5-M, 6-M, 7-M, M-NOR and M-NOR/R from the interpretation of Sichler (in Bonnin 1978). Locations of the lines are shown in Fig. 1, but their names have not been reported for sake of clarity. Approximate coordinates are as follows: Line A: (37°05'N–11°50'W)–(37°35'N–10°45'W) (TAP). Line B: (35°45'N–11°15'W)–(36°10'N–10°10'W) (HAP). Line C: (34°35'N–10°50'W)–(34°25'N–12°W) (SAP). Line D: (35°45'N–12°40'W)–(35°45'N–13°50'W) (HAP). Line M-NOR: (36°15'N–10°30'W)–(36°10'N–10°10'W) (HAP). Line 5-M: (35°50'N–11°10'W)–(36°N–10°50'W) (HAP). Line 6-M: (34°30'N–12°40'W)–(34°30'N–12°25'W) (SAP). Line 7-M: (36°55'N–12°30'W)–(36°55'N–12°50'W) (TAP). TAP: Tagus Abyssal Plain; SAP: Seine Abyssal Plain; HAP: Horseshoe Abyssal Plain.

	1st layer		1st refractor		2nd refractor		3rd refractor		4th refractor		5th refractor	
	Velocity	Thickness	Velocity	Intercept	Velocity	Intercept	Velocity	Intercept	Velocity	Intercept	Velocity	Intercept
Line A	2.0†		3.74±0.05	7.56±0.013	4.91±0.005	8.38±0.001	6.99±0.057	9.41±0.038	7.60±0.04	9.61±0.06		
Line A/R	2.0†		3.39±0.027	6.58±0.073	5.52±0.071	8.22±0.053	5.95±0.148	8.55±0.13	8.06±0.038	10.1±0.057		
Line B	2.0†		3.06±0.01	6.46±0.02	4.00±0.02	7.47±0.039	6.1±0.05	9.44±0.04	7.39±0.04	9.98±0.04		
Line B/R	2.0†		3.14±0.062	7.04±0.15	4.26±0.015	8.44±0.23	5.46±0.28	9.32±0.26	7.24±0.04	10.1±0.055		
Line C	2.0†		3.45±0.15	6.09±0.15	4.11±0.05	6.60±0.065	5.16±0.2	7.36±0.128	6.27±0.13	7.89±0.084	7.50±0.072	8.48±0.065
Line D			2.35±0.037	5.0±0.17	3.42±0.019	6.5±0.12	4.55±0.039	7.26±0.06	6.43±0.087	8.46±0.048	7.9±0.034	9.14±0.03
Line 5-M	2.10	1.18	3.12(3.56)	6.46(2.83)	3.96(3.89)	7.70(1.57)	4.81	8.74(4.76)	6.45	10.88		
Line 6-M	2.13	0.83	2.70(2.5)	5.32(0.72)	3.50(3.71)	6.2(1.45)	5.0	7.16				
Line 7-M	1.8	0.33	3.14	0.87	4.76	7.27	6.80	9.3				
Line M-NOR	1.95±0.03	0.46	2.34±0.08	0.60	4.16±0.14	4.27						
Line M-NOR/R	1.92±0.07	0.68	2.34±0.03	0.63	2.90±0.07	1.32						

very good at least as concerns the uppermost layers; the results are of course more sparse when the reflectors are deeper, but the influence of gravity modelling will also be smaller due to the increasing distance. Considering that the refraction experiments are too few to justify that we choose different velocities for each of the three abyssal plains, we decided to assign a velocity to each sedimentary unit independent of its location. The values adopted are shown in Table A3; they are mean values, except for the Cretaceous series where the velocity seemed overestimated. In Table A3, the three sets of densities picked from Nafe and Drake's plot are also shown.

APPENDIX B

Data reduction, influence of the parameters

The evolution of the anomalous signal with the successive reductions is illustrated on Fig. B1(b). The main part of the reduction is of course linked to topography (free-air anomaly/Bouguer anomaly), but the correction for the effect of sediments (Bouguer anomaly/reduced anomaly) reduces significantly the peak-to-peak amplitude of the remaining signal, and therefore the relief of the computed interface. On Fig. B1(c), the reduced anomaly has been represented for the same set of sedimentary densities but three different crustal densities; the three reduced anomalies differ noticeably: the higher the crustal density (thus the density contrast), the larger the reductions. However, even for $2.9 \times 10^3\,kg\,m^{-3}$, Gorringe Bank remains associated with a maximum of the reduced anomaly. Some sort of 'nodes' appear in the anomaly: they are obtained where the distribution of sediment layers is close to the 'mean' structure of the area. The same phenomenon can be observed in part (d) of the figure which shows the reduced anomaly for the same crustal density but three different sets of sedimentary densities. Here the minimum relative amplitude is obtained for 'low' sedimentary densities: the higher the sedimentary densities (i.e. the lower the density contrast), the lower the reductions.

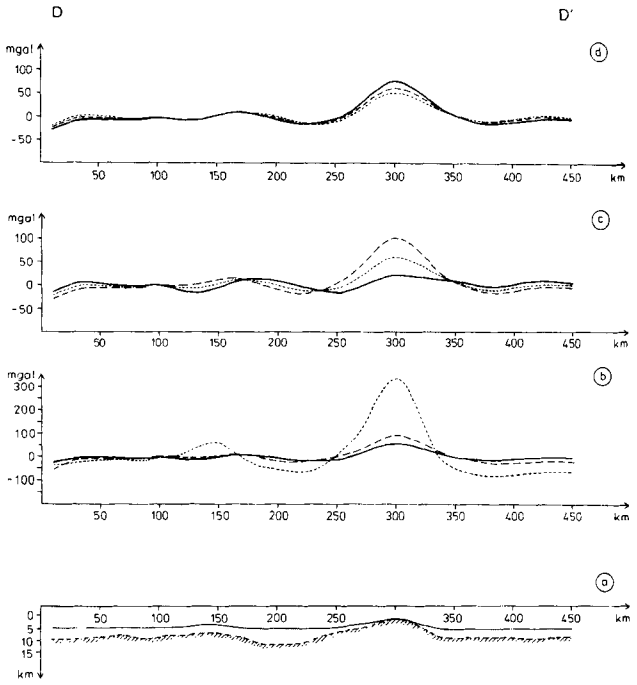

Figure B1. Section D–D' (location given in Fig. 2A). (a) *Structure* represented by the sediments (stippled) and the basement (hatched), vertical exaggeration: 2 (b) *Effect of the correction for the gravity effect of sedimentary bodies*: free-air anomaly (short dashed line), 'classical' Bouguer anomaly (long dashed line), and reduced anomaly (solid line) for a $2.7 \times 10^3\,kg\,m^{-3}$ crustal density and 'mean' values of sedimentary densities; the DC level has been removed from the Bouguer anomaly for illustrative purpose. (c) *Effect of crustal density*: reduced anomaly for 'mean' values of sedimentary densities and $2.5 \times 10^3\,kg\,m^{-3}$ (long dashed line), $2.7 \times 10^3\,kg\,m^{-3}$ (short dashed line), and $2.9 \times 10^3\,kg\,m^{-3}$ (solid line) crustal densities. (d) *Effect of sedimentary densities*: reduced anomaly for a $2.7 \times 10^3\,kg\,m^{-3}$ crustal density and 'lower' (short dashed line), 'mean' (long dashed line) and 'upper' (solid line) values of sedimentary densities picked from Nafe and Drake's plot (see Table A3).